Biophysical Chemistry 155 (2011) 20–28

Contents lists available at ScienceDirect

Biophysical Chemistry

journal homepage: http://www.elsevier.com/locate/biophyschem

Reversibility and binding kinetics of *Thermobifida fusca* cellulases studied through fluorescence recovery after photobleaching microscopy

Jose M. Moran-Mirabal *, Jacob C. Bolewski, Larry P. Walker

Department of Biological and Environmental Engineering, Cornell University, Ithaca, NY, 14853, United States

ARTICLE INFO

Article history:
Received 24 January 2011
Received in revised form 14 February 2011
Accepted 14 February 2011
Available online 19 February 2011

Keywords:
Cellulase
Fluorescence microscopy
Binding reversibility
Binding kinetics
FRAP

ABSTRACT

Cellulases are enzymes capable of depolymerizing cellulose. Understanding their interactions with cellulose can improve biomass saccharification and enzyme recycling in biofuel production. This paper presents a study on binding and binding reversibility of *Thermobifida fusca* cellulases Cel5A, Cel6B, and Cel9A bound onto Bacterial Microcrystalline Cellulose. Cellulase binding was assessed through fluorescence recovery after photobleaching (FRAP) at 23, 34, and 45 °C. It was found that cellulase binding is only partially reversible. For processive cellulases Cel6B and Cel9A, an increase in temperature resulted in a decrease of the fraction of cellulases reversibly bound, while for endocellulase Cel5A this fraction remained constant. Kinetic parameters were obtained by fitting the FRAP curves to a binding-dominated model. The unbinding rate constants obtained for all temperatures were highest for Cel5A and lowest for Cel9A. The results presented demonstrate the usefulness of FRAP to access the fast binding kinetics characteristic of cellulases operating at their optimal temperature.

1. Introduction

Cellulases are important cell-wall-degrading enzymes used in the saccharification of biomass for biofuel production [1,2]. They can be classified as endocellulases, which cleave intermediate glucosidic bonds within cellulose chains, or as exocellulases, which cleave bonds at the extremes of the chains; cellulases can also be processive, cleaving adjacent bonds in succession [1,2]. Cellulases are typically composed of a catalytic domain (CD) and one or more carbohydrate binding modules (CBMs) [1–3]. CBMs bind cellulases to cellulose [1,3] and increase the local concentration of CDs, enhancing the rate of cellulose depolymerization [4]. Consequently, understanding the effect of temperature on binding and reversibility, especially at temperatures where catalysis occurs is important to further our understanding of cellulase–cellulose interactions.

Different approaches have been used to study binding and reversibility, such as direct measurement of enzyme in solution resulting from binding equilibrium or from buffer exchange and elution with chemicals [5–8], measurement of fluorescence [9,10] or radioactive [5,11] emission resulting from exchange with labeled or unlabeled enzymes, measurement of total protein content in solution and on lignocellulose through protein hydrolysis [12], changes in refractive index measured through surface plasmon resonance [13], or mass accretion measured by quartz crystal microbalance [14,15]. Through these approaches, cellulase binding kinetics have been addressed for different cellulosic substrates such as filter paper [13], Avicel [5–7,12], pretreated corn stover [12], wood [11], and native [5,7–10,16] and reconstituted [14,15] bacterial micro-crystalline cellulose (BMCC). Overall these studies have found that cellulases bind tightly and competitively to cellulose at low temperatures, while binding strength is reduced and can become synergistic at higher temperatures. On the other hand, studies on binding reversibility have found that temperature, substrate accessibility, and type of catalytic activity influence the binding kinetics. As a result, the quantification of binding reversibility has yielded inconsistent results, with studies reporting cellulase binding as either reversible, partially reversible, or completely irreversible [5,6,8,11–13]. In addition, most studies on cellulase binding have been performed by indirect measurements, which has limited the spatial and temporal resolution, and has given limited access to the effect that temperature and cellulose structure have on binding and reversibility. Thus, methods that quantify binding and reversibility of cellulases in real time, detailing the complexity of cellulose structures, at relevant temperatures, and with high spatio-temporal resolution could greatly expand our understanding of cellulase–cellulose interactions.

In previous work, our group has utilized fluorescently-labeled *T. fusca* cellulases in combination with surface-immobilized BMCC to demonstrate the high spatio-temporal resolution achieved for binding assays through quantitative fluorescence microscopy [17]. In the present study we build on our previous work by implementing Fluorescence Recovery After Photobleaching (FRAP) microscopy for

* Corresponding author at: 230 Riley-Robb Hall, Cornell University, Ithaca, NY 14850, United States. Tel.: +1 607 255 5544.
E-mail addresses: jmm248@cornell.edu (J.M. Moran-Mirabal), lpw1@cornell.edu (L.P. Walker).

0301-4622/$ – see front matter © 2011 Elsevier B.V. All rights reserved.
doi:10.1016/j.bpc.2011.02.003

the study of cellulase binding and reversibility on surface-immobilized BMCC. FRAP probes the recovery of fluorescence due to the molecular transport of labeled molecules into an area where fluorescence has been bleached by a high-intensity illumination pulse [18–20]. Depending on the system studied, recovery can stem from diffusion or from active binding and unbinding [20,21]. Thus, fitting the FRAP recovery curves to diffusion and/or binding models can reveal kinetic details on the behavior of the fluorescent species [18–22]. In the past, Jervis and collaborators used FRAP to assay the surface diffusion of cellulases and their isolated CBMs on cellulose sheets [23]. In this study binding kinetics were not targeted, and the effect of binding/unbinding on the observed recovery was intentionally minimized by extensive washing and the addition of a second cellulose sheet as a sink for unbound cellulases and CBMs. However, FRAP can also be employed to measure protein binding kinetics, making it ideally suited to study cellulase binding and binding reversibility on cellulosic materials.

The goal of the present study was to elucidate the binding kinetics and binding reversibility, at a range of temperatures, for *T. fusca* cellulases adsorbed onto BMCC through FRAP microscopy. For our experiments we selected cellulases Cel5A (a classical endocellulase), Cel6B (a processive exocellulase), and Cel9A (a processive endocellulase). The choice of this set of cellulases builds on our expertise and is representative of the distinct modes of catalysis found both in fungal and bacterial cellulases. Our results show that binding for these cellulases at all temperatures is only partially reversible. Furthermore, the fraction of enzymes reversibly bound to cellulose was independent of temperature for the classical endocellulase Cel5A, while it decreased with increasing temperature for processive exocellulase Cel6B and processive endocellulase Cel9A, which suggests a strong relationship between catalysis and binding reversibility. Kinetic binding parameters were obtained by fitting FRAP curves to a binding-dominated model. The unbinding rate constants obtained for all temperatures were highest for Cel5A and lowest for Cel9A. In addition, all cellulases showed higher apparent dissociation constants at higher temperatures. The results presented demonstrate the usefulness of FRAP microscopy to study binding reversibility and access the fast binding kinetics characteristic of cellulases operating at their optimal temperature.

2. Materials and methods

2.1. Cellulase production and labeling

T. fusca cellulases Cel5A, Cel6B, and Cel9A were expressed and purified as described by Jeoh [10] and Jung [24]. They were labeled with Alexa Fluor 488 (Invitrogen, Carlsbad, CA) using a solid-phase protocol and FPLC purified as previously reported [25]. Only cellulases with degree of labeling of one and exhibiting full hydrolytic activity on BMCC were used in FRAP experiments.

2.2. Sample preparation

A stock suspension of BMCC (Monsanto Cellulon, San Diego, CA) was prepared as previously described [9,10]. A 50 μg/ml BMCC suspension in MilliQ water was sonicated for 5 min at 60% amplitude using a SPLt sonicator (Branson, Danbury, CT). Then, 10 μl of the suspension were spread on a 40 mm, 170 μm thick glass wafer (Bioptechs, Butler, PA) previously treated using a Plasma Cleaner (Harrick, Ithaca, NY). A droplet of the BMCC solution was spread across the glass and dried at 70 °C for 5 min; the glass was then used to create a fluidic chamber (Supplemental Fig. 1, FCS2 chamber assembly, Bioptechs, Butler, PA). The sample was rinsed with MilliQ water and incubated for 4 h with 10% BSA (Fisher Scientific, Pittsburgh, PA). Then, it was rinsed with 40 ml of imaging buffer (50 mM sodium acetate buffer, 5 mM ascorbic acid, pH 5.5), and rehydrated overnight. Prior to imaging, 2.5 ml of 2 nM cellulase solution in imaging buffer were incubated with the sample for 1 h at 4 °C for binding, after which an additional 2.5 ml of cellulase solution was perfused in, yielding a total of 20 μmol enzyme/gram BMCC in the sample. The sample was finally mounted on the microscope, where temperature was held constant by resistive heating provided by the FCS2 and an objective heater.

2.3. Confocal imaging and FRAP

BMCC-bound cellulases were imaged using an Olympus IX81-FV1000 confocal microscope (Olympus, Center Valley, PA) equipped with laser excitation at 405 and 488 nm and a PLAPO 60X/1.45NA TIRFM oil immersion objective. All imaging was performed at 1.5% 488 nm laser power, gain = 1, photo multiplier tube (PMT) voltage = 300–650, 20 μs pixel (px) dwell time, 8× zoom, and confocal aperture of 100 μm. In FRAP experiments, two reference images were taken, then selected areas were bleached (100% 405 nm laser, 40 μs px dwell time), and recovery images were taken at 3–30 s intervals. Images were corrected for stage drift using the Stackreg plugin [26] for ImageJ (NIH, Bethesda, MD), and pre-processed using a custom Matlab routine (Mathworks, Natick, MA). This routine allowed the user to select a background area and establish a threshold based on the mean background intensity and standard deviation. The threshold was used to separate pixels that were considered signal (fluorescence coming from cellulases bound to cellulose) and those that were considered background (areas devoid of cellulose). At the same time, saturated pixels were removed from further analysis. Finally, the mean background was substracted form the entire image. This pre-processing yielded images where the intensity for background and saturated pixels was set to zero and the intensities for signal pixels accurately reflected the amount of bound cellulases.

FRAP images were analyzed using a program developed in Python (www.python.org), that located the bleached areas by a user-defined threshold on the change of intensity between the pre-bleach images and the first recovery image. The threshold was set to 25% for FRAP on fibrils and 50% for mats to match the areas programmed for bleaching. An exclusion region was created for all bleached areas to eliminate pixels at the boundary of the bleached area that are only partially bleached. All signal pixels outside the exclusion regions were used as reference to correct for photobleaching during the time-lapsed recovery. Finally, the average intensity of each bleached area was normalized to the reference intensity, and recovery curves were constructed. All recovery curves for a particular experimental condition were averaged ($n \geq 5$) and fitted to the binding/unbinding model (described below) using a non-linear Levenberg–Marquardt curve fitting approach in OriginPro8 (OriginLab, Northampton, MA). All values reported for the fitted parameters are presented with the propagated errors containing the variation between experimental replicates and uncertainties from the fitting.

2.4. Fluorescence calibration

Fluorescence intensity was calibrated to cellulase concentration through serial dilutions of Alexa488-dUTP (Invitrogen, Carlsbad, CA). Three images were acquired for each temperature, PMT HV setting, and dUTP concentration. Average pixel intensities were plotted against concentration and the slope (α) was estimated by linear regression (Supplemental Fig. 2). Plots of α against HV yielded calibration curves for each temperature (Supplemental Fig. 3).

2.5. Cellulase binding/unbinding FRAP model

FRAP curves were fitted to a model [21], where recovery is dominated by the kinetics of cellulase binding to cellulose:

$$\frac{dC_B}{dt} = k_{on} C_F S - k_{off} C_B \quad (1)$$

where C_F is the concentration of cellulase in solution, S is the concentration of available binding sites on the cellulose surface, C_B is the bound cellulase concentration, and k_{on} and k_{off} are the binding and unbinding rate constants. Assuming no quenching, Eq. (1) can be multiplied by α, which relates bound cellulase concentration to fluorescence intensity I_B, to yield:

$$\frac{dI_B}{dt} = k_{on}^{*} C_F \alpha - k_{off} I_B \tag{2}$$

where k_{on} has also been replaced with an apparent binding rate constant $k_{on}^{*} = k_{on} S$.

Bleaching a small fraction of the fluorescent molecules in FRAP experiments disturbs the distribution of fluorescent and non-fluorescent molecules, but does not alter the equilibrium between bound and unbound molecules [21]. Thus, through FRAP it is possible to measure binding reversibility and binding kinetics in a system under equilibrium conditions, such as those obtained after prolonged incubation of the cellulases with BMCC. In this case, the term $k_{on}^{*} C_F \alpha$ is constant and Eq. (2) can be directly integrated, using the initial condition $I_B(0) = 0$. This yields the following equation:

$$I_B(t) = \frac{k_{on}^{*} C_F \alpha}{k_{off}} \left(1 - e^{-k_{off} t}\right) = F_M \left(1 - e^{-k_{off} t}\right) \tag{3}$$

where F_M is the mobile fraction (fraction of cellulases reversibly bound). It must be noted that in a system where the substrate can change as a result of catalytic action of the bound molecules, such as the cellulose–cellulase system, FRAP can still be used to study binding kinetics as long as the FRAP observation window is much smaller than that of the overall degradation of the substrate, and the system can be considered in quasi-equilibrium. This is an assumption that holds for the cellulase–cellulose system, where the degradation of the substrate by nanomolar concentration of cellulases takes place over the course of hours and the FRAP observation window is on the order of minutes.

3. Results and discussion

3.1. Cellulose immobilization and cellulase binding

The sample preparation yielded a distribution of cellulose morphologies from dense cellulose mats (Fig. 1a–b) to single fibrils (Fig. 1c), which we henceforth describe following nomenclature previously reported [17]. Fibrils had widths below the microscope's diffraction-limited resolution (<200 nm), lengths in microns, and in the axial dimension were confined to a single confocal plane (350 nm slice). On the other hand, mats had sizes of tens of microns, dense fibrilar structure, and were 1–2 μm thick, spanning multiple confocal planes (Supplemental Fig. 4).

Fluorescence intensities of BMCC-bound cellulases were converted into concentration plots (Fig. 1b–c) using the calibration curves (Supplemental Figs. 2 and 3). Concentration plots at 23 °C were chosen to compare the binding behavior of *T. fusca* cellulases because at this temperature they exhibit little hydrolytic activity (<15% of that at 50 °C). It must also be noted that because mats were thicker than a confocal plane, each imaged voxel (three dimensional pixel) is entirely filled with BMCC and the concentration plots accurately show the amount of cellulase bound on cellulose. On the other hand, fibrils with diameters in the 10–50 nm range [27–29] are thinner than a single confocal plane, which results in an underfilled voxel. This leads to an underestimation of the concentration of the enzymes bound on the cellulose fibrils.

Analysis of the concentration plots at 23 °C (Fig. 1c) revealed that the concentration of BMCC-bound cellulases was in the micromolar range (which for a completely filled voxel translates into nanomoles per gram BMCC, Table 1). The distribution of the enzymes on cellulose fibrils was relatively homogeneous, in agreement with the random binding of CBMs to the available cellulose surfaces. The plots for dense BMCC mats showed that Cel5A and Cel6B bound in comparable concentrations, while Cel9A showed lower values (Fig. 1b and Table 1). The concentrations were consistent over a number of mats, ruling out the possibility that the differences between Cel5A, Cel6B, and Cel9A binding were due to different substrate density or composition. The observed variations in the amounts of bound enzymes are most likely due to different binding affinity, cellulase size, and the relative accessibility to the interior cellulose structure of mats, where interstitial space, pores and crevices between fibers, can have dimensions comparable to those of cellulases [30] and hinder the diffusion of enzymes on the basis of their hydrodynamic radius. The hydrodynamic radii of Cel5A and Cel6B have been measured through dynamic light scattering to be ~4 nm, while Cel9A has been found to behave like an ellipsoid with minor and major axes of ~5 and 11 nm (unpublished results), which would explain why Cel9A shows lower concentrations of bound cellulases on mats. Concentration plots were also obtained at 34 and 45 °C (Table 1, Supplemental Figs. 5 and 6). Overall, as temperature increased, the concentration of bound enzymes decreased, which is attributed to a higher dissociation constant and increased hydrolytic activity. Further experiments with inactive cellulases or individual CBMs at saturating conditions could allow a direct estimation of the influence of saturation and temperature on binding without catalysis.

3.2. Impact of bleached area size and cellulose morphology on recovery

To assess binding reversibility and obtain the kinetic binding constants FRAP experiments were conducted with Cel5A, Cel6B, and Cel9A cellulases bound to cellulose mats and fibrils. The fluorescence recovery observed (Fig. 2a–b) was attributed solely to the replacement of bleached enzymes that unbound from the cellulose with fluorescent ones from the bulk solution. This assumption is justified because the experiments were conducted under equilibrium conditions and no sustained surface diffusion has been observed under the experimental conditions used (unpublished single molecule data, e.g. Supplemental Videos 1–3). FRAP curves for the bleached areas in all replicate experiments ($n \geq 5$) were pooled together and averaged for each experimental condition. The averaged curves were fitted to the binding-dominated FRAP model (Eq. (3)) to obtain the kinetic binding constants.

The effect of bleached area size on the recovery curves was assessed for both cellulose fibrils and mats. The diameter of the circular bleached areas was varied between 10 and 50 px for fibrils. No significant difference in recovery was observed between these bleached areas, which further supports the lack of a diffusion component in the recovery. Consequently, the bleaching diameter for experiments on fibrils was fixed at 20 px (Fig. 2a and c). The lack of variation of recovery with bleached area size on individual cellulose fibrils was an expected result, since the bulk solution contained free enzymes, and recovery was dominated by the binding/unbinding turnover. On the other hand, varying the size of bleached areas on mats (Fig. 2b) resulted in significant differences in recovery (Fig. 2d–e). Thus, two bleached area sizes were chosen for subsequent FRAP experiments on mats: circles with 10 px diameter (henceforth referred to as small areas) and 50 px side squares (large areas). These dimensions were chosen to mirror those used in previously published FRAP experiments for *Cellulomonas fimi* cellulases [23].

Previous experiments have reported cellulase binding at room temperature to be anywhere from irreversible to completely reversible [5,6,11–13,16]. Our FRAP experiments conducted on *T. fusca* cellulases Cel5A, Cel6B, and Cel9A bound to BMCC fibrils and mats (Fig. 3) provide direct evidence that cellulase binding and unbinding is very dynamic with recovery times on the order of minutes, and only partially reversible. From Fig. 3 it is observed that for all cellulases the recovery on mats is significantly slower than the recovery on fibrils, and that the recovery on mats for large bleached areas is significantly slower than for small areas. The differences in

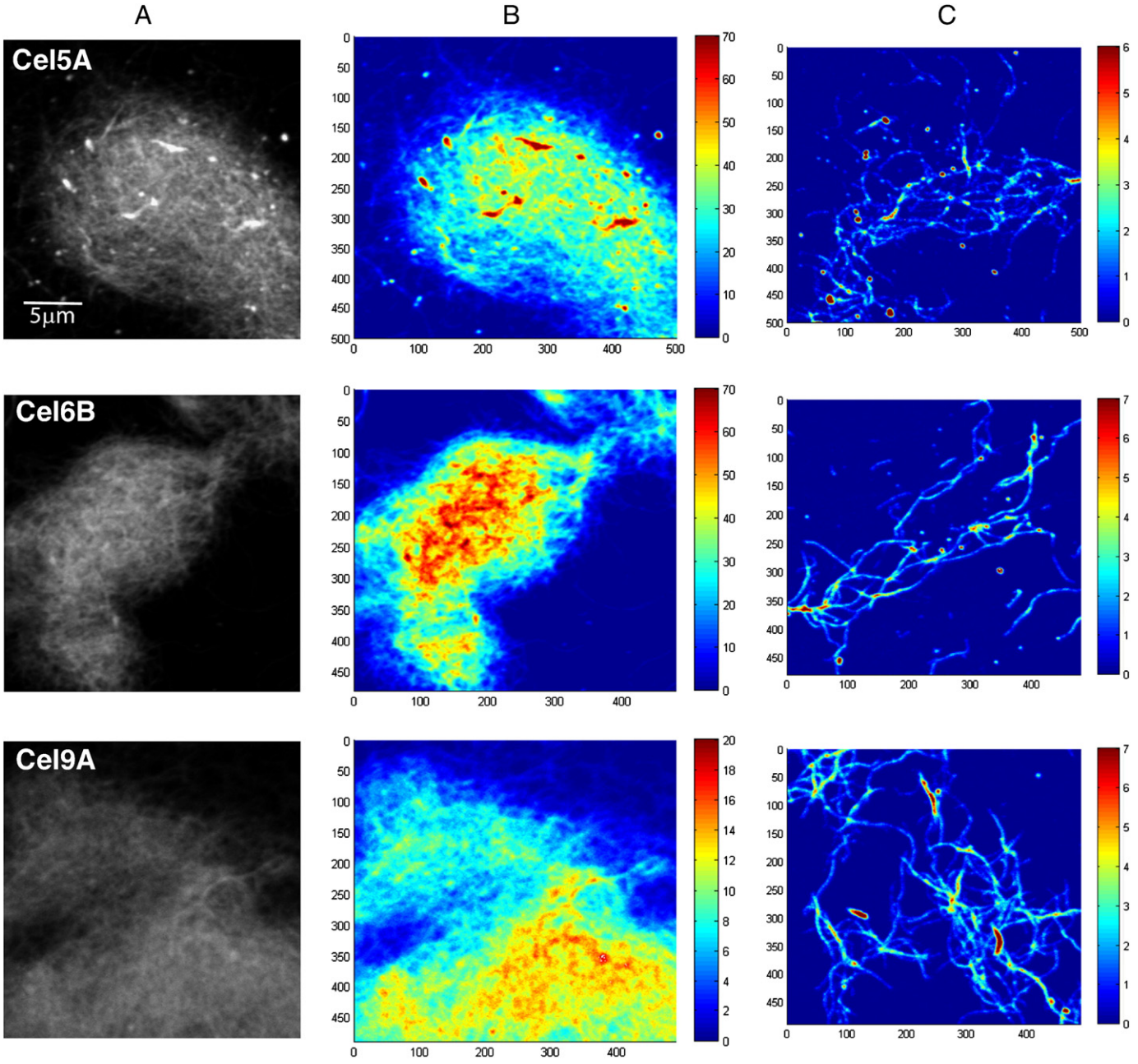

Fig. 1. Conversion of fluorescence images to local concentrations of bound enzyme on BMCC. (A) Fluorescence intensity images taken for cellulases Cel5A, Cel6B, and Cel9A bound on dense cellulose mats at 23 °C. (B) Local concentration maps for the images in (A). (C) Local concentration maps for individual fibrils. The concentrations values (color bar) are presented in micromolar, and the values for the x–y axes are in pixels (51 nm/px).

recovery rate between mats and fibrils were attributed to cellulose accessibility and to hindered bulk diffusion. In the case of cellulose fibrils, all surface area available is equally accessible and no diffusion hindrance is expected, leading to similar recovery curves from different-size bleached areas. Furthermore, the fibrils are disperse enough that unbinding of enzymes and rebinding to neighboring fibrils is highly unlikely. On the other hand, mats have a porous structure where cellulose in deep layers is not as accessible as that on

Table 1
Range of local bulk concentrations of bound cellulases on BMCC given in μM (and in parentheses in nanomol cellulase per gram BMCC), estimated from calibrated confocal fluorescence microscopy images. Estimates of the amount of cellulase per gram BMCC were obtained (only for dense mats where BMCC completely fills the voxel) assuming a bulk density of 1.5 g/cm^3 for BMCC [23,31].

Temperature	23 °C		34 °C		45 °C	
BMCC structure	Dense mats	Fibrils	Dense mats	Fibrils	Dense mats	Fibrils
Cel5A	20–50 (13–33)	1–4	5–15 (3–10)	0.5–2	3–9 (2–6)	0.5–2.0
Cel6B	20–60 (13–40)	2–5	15–40 (10–27)	1–3	15–35 (10–23)	0.5–2.5
Cel9A	5–15 (3–10)	2–5	5–10 (3–7)	0.5–2.5	3–9 (2–6)	0.5–2.5

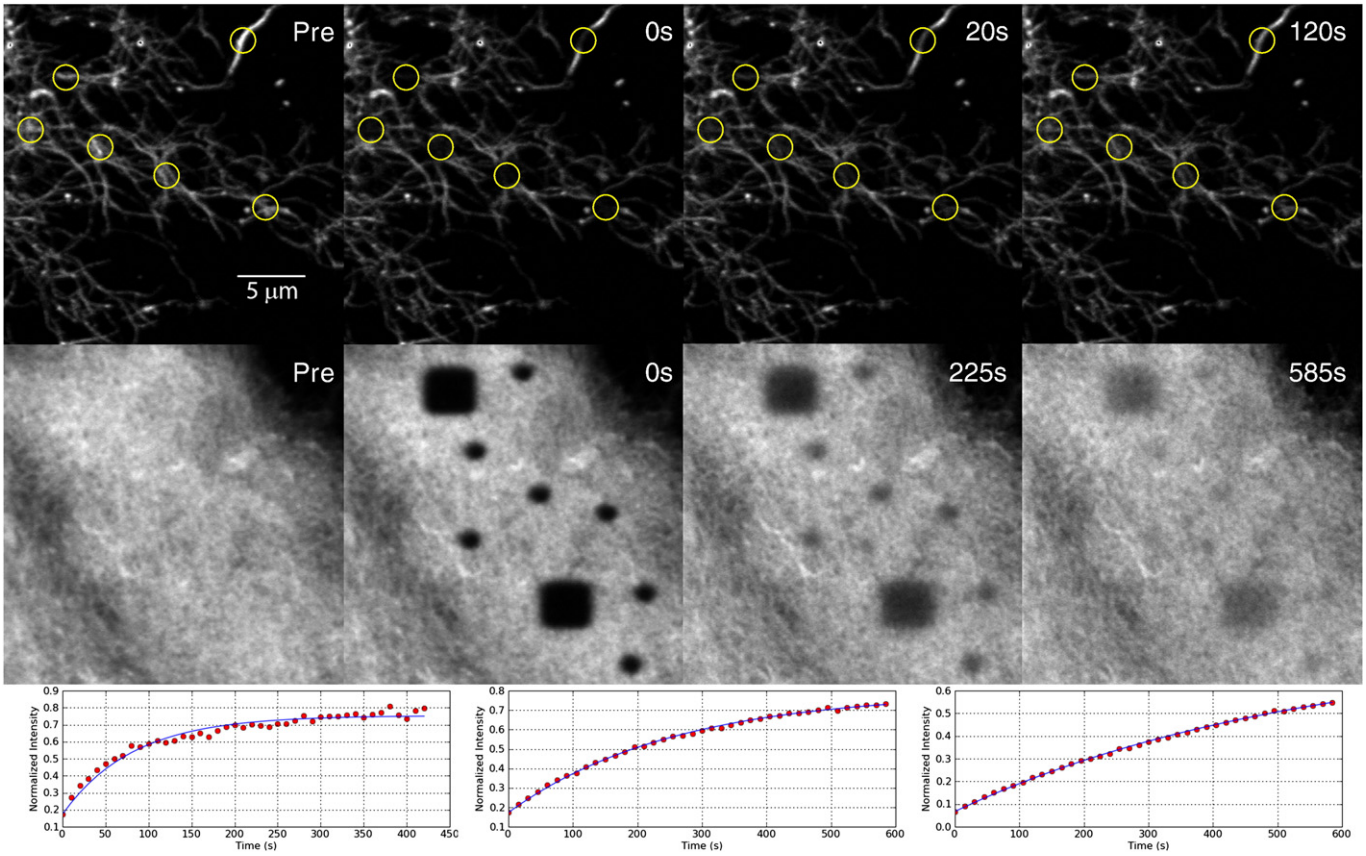

Fig. 2. Sample images from FRAP experiments performed on Cel9A cellulases bound onto BMCC structures at 23 °C. All fluorescence images shown at the same magnification. (a) Images depicting bleached areas (circles, 20 px diameter) and their recovery on individual cellulose fibrils. Pre-bleaching image (Pre) was used to normalize the recovery images. (b) Images depicting bleached areas (circles 10 px diameter, squares 50 px side) and their recovery on dense cellulose mats. Sample recovery curves (dots) for bleached areas on individual fibrils (c), and small (d) and large (e) bleached areas on dense cellulose mats, and their corresponding fits to the recovery model (solid lines).

the external surface. This leads to longer recovery times because binding and diffusion through the interstitial spaces occur within the mats. In addition, the concentration of bound cellulases surrounding the bleached areas in mats is high and may significantly contribute to local rebinding events especially in deep cellulose layers, which would explain the variations in recovery for different-size bleached areas.

3.3. Effect of temperature on reversibility

The effect of temperature on cellulase binding and reversibility was studied through experiments at 23, 34, and 45 °C (Fig. 4).While the optimal temperature for hydrolysis for *T. fusca* cellulases is 50 °C, the temperature in our experiments was limited to a maximum of 45 °C to preserve the integrity of the microscope objective. As shown by the error bars in Fig. 4, bleaching experiments were highly reproducible within and across independently-prepared samples for all enzymes. However, it was found that the longer the sample was incubated with Cel9A at temperatures where significant hydrolysis occurred, the lower the value for the maximum fluorescence recovered. This was attributed to Cel9A's high hydrolytic activity on crystaline cellulose, as compared to other *T. fusca* cellulases [32]. To minimize changes due to hydrolysis, subsequent experiments for Cel9A at each of the studied temperatures were conducted with freshly prepared BMCC samples.

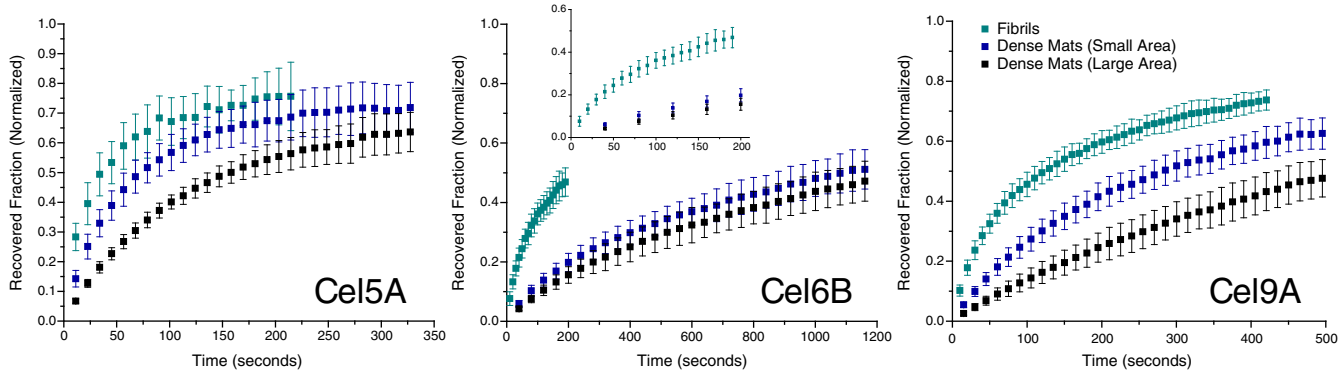

Fig. 3. Comparison of the averaged FRAP recovery curves for different cellulose structures. Experiments were conducted at 23 °C. Recovery curves for fibrils are presented in light green, for small bleached areas on dense mats in blue, and for large bleached areas on dense mats in black. Curves are averages of recovery curves for individual bleached areas (n = 5–30). Error bars represent the standard deviation from the different recovery curves. Inset graph for Cel6B presents a zoomed in view of the average recovery curve for fibrils.

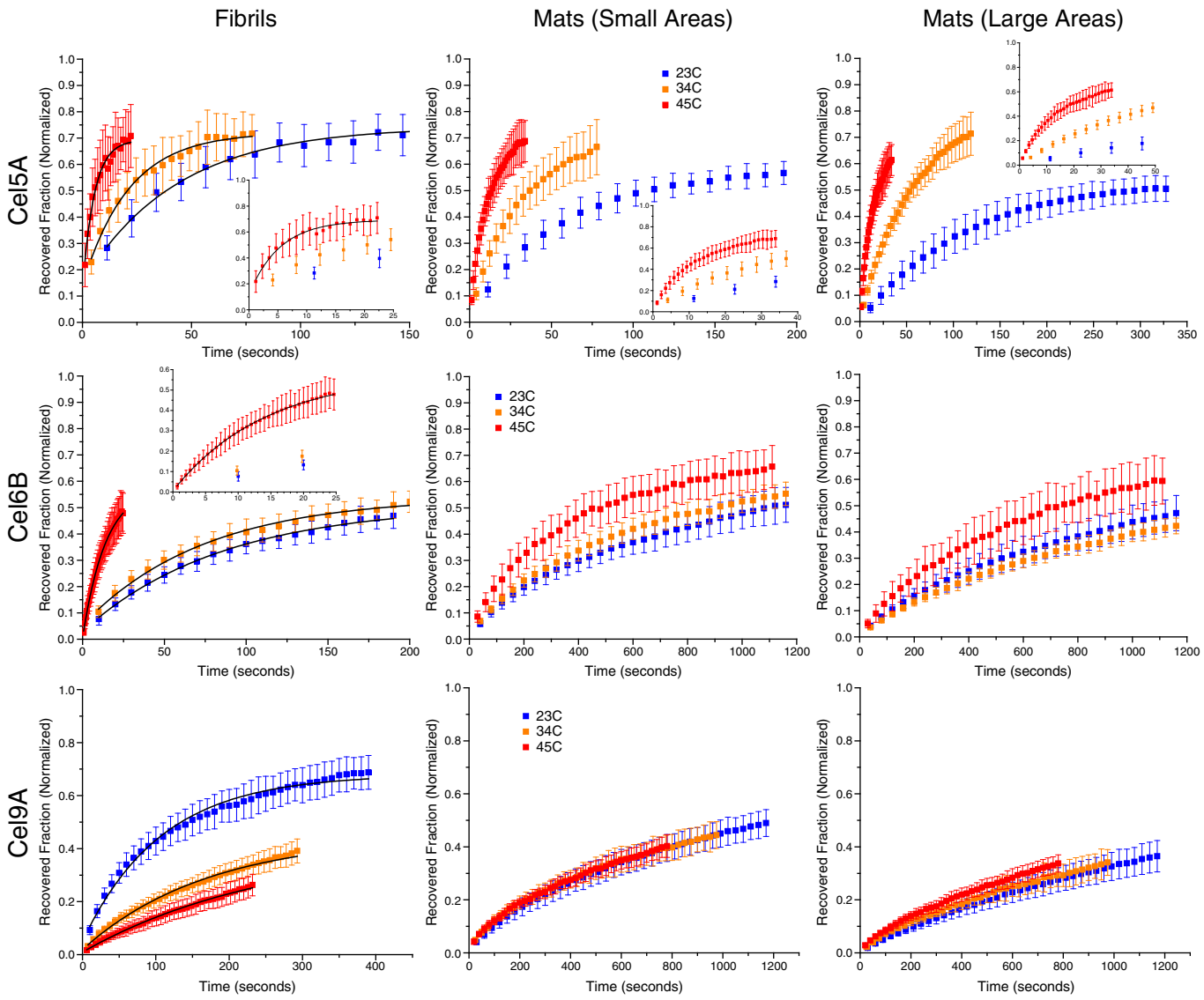

Fig. 4. Comparison of the averaged FRAP recovery curves for different temperatures on the different cellulose structures. Recovery curves for 23, 34 and 45 °C are presented in blue, orange and red respectively. Curves are averages of recovery curves for individual bleached areas (n = 5–30). Error bars represent the standard deviation of the different recovery curves. Insets present zoomed views of the average recovery curves at 45 °C. Fits to the binding dominated model (Eq. (3)) are shown in black for fibril data only.

Qualitatively, Fig. 4 shows that for Cel5A an increase in temperature accelerated the recovery, while it had little effect on the maximum fluorescence recovered. For Cel6B, only the increase from 34 to 45 °C significantly accelerated the recovery, while the maximum fluorescence recovered was slightly reduced with each temperature increase. For Cel9A it was hard to qualitatively assess whether the recovery was faster at higher temperatures. However, from information obtained from experiments performed on fibrils, it is evident that as temperature increased, the maximum fluorescence recovered decreased. From these results it is observed that Cel5A and Cel6B followed the expected behavior, where an increase in temperature accelerates the recovery, leading to a higher turnover rate, while Cel9A did not.

The averaged recovery curves for fibrils (Fig. 4) were fitted to the binding-dominated FRAP model (Eq. (3)) to extract the cellulase binding parameters. Experiments performed on fibrils were selected for fitting because they allow a simplified analysis that need not take into account interstitial space entrapment and diffusion hindrance encountered in cellulose mats. In addition, the use of data from fibrils justifies the use of Eq. (3) to account for recovery, since previous studies have shown that cellulase binding to isolated fibrils adjusts well to a Langmuir binding model with a limited number of available binding sites [17]. Fitting of the experimental data to the binding-dominated model (*e.g.* Fig. 5a, red line) yielded values for F_M (mobile fraction, dashed blue line), k_{off}, and k^*_{on}. F_M is a measure of cellulase binding reversibility and represents the fraction of cellulose-bound enzymes that can be replaced by fluorescent enzymes from solution, while $1 - F_M$ yields the fraction of immobile cellulases. Fig. 5b shows the F_M values for FRAP experiments on fibrils at different temperatures. It is observed that all three cellulases exhibit only partial reversibility, which is consistent with previous reports [4,8,16]. However, because in these experiments the mobile fraction is obtained directly from measurements on fibrils, irreversibility cannot be attributed to interstitial space entrapment. Thus, the irreversible binding observed can only arise from cellulase–cellulose fibril interactions, and a decrease in F_M can only be explained by the irreversible attachment of enzymes to the cellulose surface.

Comparing the mobile fractions obtained at 23 °C (Fig. 5b) reveals that all cellulases exhibit the same extent of reversibility, suggesting that when there is little catalysis, reversibility is primarily determined by CBM binding. This agrees with previous observations that binding of cellulase mixtures at low temperatures is dominated by the CBMs

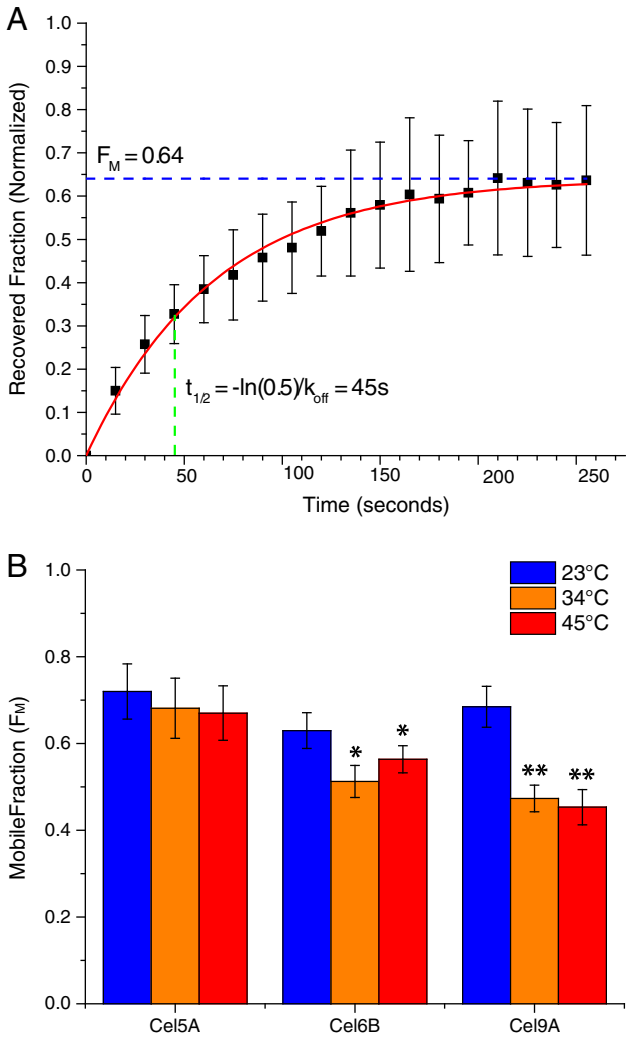

Fig. 5. Reversibility of *T. fusca* cellulases Cel5A, Cel6B, and Cel9A binding assessed by FRAP. (A) The averaged recovery curve for Cel6B bound on BMCC fibrils at 23 °C is shown in black and its fit to the recovery model is shown in red, with F_M and $t_{1/2}$ values presented as dashed lines. (B) Mobile fraction of bound cellulases extracted from the averaged recovery curves. Error bars represent standard deviation from multiple bleaching experiments ($n \geq 5$). (*) and (**) represent statistical significance at 0.95 and 0.99 confidence respectively, when compared to measurements with the same enzyme at 23 °C.

and results in competitive binding [8,10]. Fig. 5b also shows that as temperature is increased, F_M remains constant for Cel5A, but decreases for Cel6B and Cel9A. The fact that a decrease in F_M is seen only for processive enzymes, suggests a relationship between the catalytic activity of the cellulase and the fraction that can dissociate from the cellulose. As mentioned earlier, Cel5A is a classical endocellulase that randomly cleaves glucosidic bonds along the cellulose polymer. Thus, the binding-catalysis cycle of Cel5A does not require the cellulase to remain attached to the cellulose through its CD and the enzyme can readily dissociate. In comparison, exocellulase Cel6B cleaves glucosidic bonds in a processive fashion; while processive endocellulase Cel9A initially cleaves a random glucosidic bond but then continues cleaving neighboring bonds in succession. Both processive enzymes follow the same initial binding and catalysis steps as Cel5A, but instead of unbinding after catalysis, they remain attached to the cellulose through their CD and continue cleaving glucosidic bonds. Our results suggest that the sustained association of the CD with the cellulose chain makes processive cellulases more likely to bind irreversibly during catalysis. It has been previously shown that binding of CDs by themselves is less reversible than that of whole cellulases [8], which supports the notion that the irreversibility at temperatures where catalysis occurs is due to the specific CD–cellulose interaction.

3.4. Effect of temperature on binding constants

Fitting of the averaged FRAP curves to the binding dominated model (Eq. (3)) yielded the rate constants for cellulase binding. It is important to note that the k_{off} values are determined solely by the temporal evolution of the recovery, and do not depend on the reversibly bound fraction (F_M). On the other hand, k_{on}^* values are intrinsically tied to F_M and to the available binding sites (S) on the cellulose surface. Thus, k_{off} represents a true unbinding rate constant, while k_{on}^* represents an apparent binding rate constant, and could be affected by the fraction of immobilized enzymes. This distinction becomes important when interpreting the observed behavior, especially in the case where the mobile fraction changes as a function of temperature. Table 2 presents the k_{off} values obtained for the different temperatures assayed. It is observed that as temperature is increased, k_{off} increases for both Cel5A and Cel6B, indicating a shorter time spent by the enzymes in the bound state. In contrast, Cel9A shows a decrease in k_{off} as the temperature is increased, implying longer residence time by the enzyme in the bound state. From k_{off}, the half-recovery time can be calculated as $t_{1/2} = -\ln(0.5)/k_{off}$, which serves as an indicator of how quickly the turnover of bleached enzymes occurs, with shorter $t_{1/2}$ corresponding to faster recovery. $t_{1/2}$ for Cel5A and Cel6B decreased from 23 to 2 and from 45 to 9 s respectively as temperature increased from 23 to 45 °C, while $t_{1/2}$ for Cel9A increased from 77 to 201 s. It is observed that Cel5A and Cel6B again conform to the expected behavior of higher k_{off} as temperature is increased, while Cel9A deviates from it. This behavior could be attributed to Cel9A's higher catalytic activity as compared to the other cellulases, and the modification of the available binding sites in the underlying substrate.

Values for k_{off} and k_{on}^* were used to calculate an apparent dissociation constant $K_D^* = \frac{k_{off}}{k_{on}^*}$. The influence of temperature on the apparent dissociation constant is shown in Table 2. For all three cellulases K_D^* increases with increasing temperature. This result implies that at higher temperatures, higher enzyme concentrations are required to achieve half saturation of the available binding sites. It is interesting to note that for Cel9A, although k_{off} decreases with increasing temperature, the apparent binding rate constant ($k_{on}^* = k_{on}S$) decreases to an even greater extent (due to a decrease in both the available binding sites and the true binding rate constant), ultimately resulting in an increase in K_D^*. This further supports the notion that hydrolysis of the substrate by Cel9A changes the binding landscape that the cellulases encounter. In binding experiments where no catalytic activity is involved, an increase in temperature typically leads to an exponential increase in K_D^* which allows the calculation of the characteristic binding energy of the system. With cellulases the binding behavior at high temperatures is convolved with the hydrolytic activity and the fraction of enzymes that bind irreversibly. Thus, the increase in K_D^* cannot be directly correlated to the binding energy for the cellulose–cellulase system. As a final exercise, if a true dissociation constant (K_D) is calculated using the k_{off} values

Table 2
Kinetic rates extracted from average FRAP recovery curves for *T. fusca* cellulases bound to BMCC fibrils for the different temperatures assayed. Errors reported represent the propagated error corresponding to the variations between experimental replicates and curve fitting to the model.

Temperature	23 °C		34 °C		45 °C	
Kinetic parameter	k_{off} 10^{-3} (s^{-1})	K_D^* 10^{-4}	k_{off} 10^{-3} (s^{-1})	K_D^* 10^{-4}	k_{off} 10^{-3} (s^{-1})	K_D^* 10^{-4}
Cel5A	34 ± 2	2.8 ± 0.2	76 ± 6	4.5 ± 0.4	263 ± 16	5.1 ± 0.4
Cel6B	15.3 ± 0.7	2.1 ± 0.1	17.7 ± 0.9	4.4 ± 0.3	75 ± 2	6.1 ± 0.1
Cel9A	8.9 ± 0.4	2.4 ± 0.1	5.2 ± 0.3	6.5 ± 0.4	3.4 ± 0.2	7.5 ± 0.6

obtained from the FRAP experiments reported here, together with the k_{on} (true binding rate constant) values reported in the literature for the same *T. fusca* cellulases [17], we find dissociation constant values in the 10–50 nM range. These values are lower than K_D values reported from measurements performed in bulk [5,33], meaning that we observe tighter cellulase–cellulose binding. This difference could arise because the rate constants were derived from temporal measurements from individual fibril adsorption/desorption isotherms, and not from an average of all cellulose structures. However, to get definitive true dissociation constant values the adsorption/desorption experiments should be performed on the same fibrils.

4. Conclusions

FRAP experiments were performed on *T. fusca* cellulases Cel5A, Cel6B, and Cel9A bound onto BMCC fibrils and mats to assay binding reversibility and kinetics at different temperatures. Our results show that, under the experimental conditions used, cellulases bind to cellulose fibrils and mats with concentrations in the nanomol per gram BMCC range, well below its maximum binding capacity.

Cellulase binding reversibility was quantitatively assessed through the mobile fraction. The results unequivocally show that cellulase adsorption is only partially reversible, and that the mobile fraction depends strongly on the type of cellulase and temperature. It was observed that at room temperature, where there is minimal catalytic activity, the mobile fraction was similar for all three cellulases (*ca.* 70%), while at elevated temperatures the behavior was different between processive and non-processive cellulases. This suggests that at low temperature binding is determined mostly by CBM-cellulose interactions. As temperature was increased the mobile fraction remained unchanged for classical endocellulase Cel5A, while it was reduced for processive cellulases Cel6B and Cel9A. This indicates that processive enzymes have a higher immobile fraction at temperatures where there is significant interaction between the CD and the cellulose. Our results as a whole imply that some of the observed loss of catalytic activity during cellulose depolymerization is caused by cellulases adsorbing irreversibly onto cellulose. An explanation for the higher immobile fraction for processive cellulases is that these enzymes encounter physical barriers during catalysis which prevent them from continued processivity. These enzymes would not be able to dissociate from the cellulose chain because it is threaded into their CD, thus remaining immobilized on the surface. In this scenario, mixtures which combine endocellulases and exocellulases would result in the release of some of the immobile enzymes, and enhance the hydrolytic activity through synergism.

The unbinding rate constants extracted from recovery curves evidenced further differences between the cellulases. It was found that with higher temperatures k_{off} increased for Cel5A and Cel6B, but decreased for Cel9A. Typically, upon heating the added thermal energy causes ligands to unbind more readily from their targets, leading to higher unbinding rates and dissociation constants. Our results show that Cel5A and Cel6B behave in this fashion, while Cel9A does not. While the reason for this behavior is unclear, it indicates that Cel9A cellulases spend more time bound to cellulose at temperatures where catalysis occurs. Finally, it was observed that for all the cellulases the apparent dissociation constant increased upon increasing the temperature. This was the expected behavior for all enzymes, regardless of the observed anomalies in the behavior of Cel9A. However, the fact that the apparent dissociation constant increases for Cel9A despite a lower unbinding rate constant, means that the apparent binding rate constant must decrease at an even faster rate. This can only be explained if the number of available binding sites decreases due to hydrolysis.

In summary, the binding kinetics of *T. fusca* cellulases have been probed as a function of temperature through FRAP. These experiments have shed light on the binding reversibility of these cellulases, the effect of temperature, and of the inherent cellulose structure. Anomalous behavior was observed for Cel9A, a processive endocellulase, which can be explained by the assumption that processive enzymes can stall during hydrolysis. This highlights the value of high spatial and temporal resolution in binding assays, because equilibrium measurements of dissociation constants can mask some of the mechanistic behavior of these enzymes.

Acknowledgements

This research made use of equipment and facilities from the Biofuels Research Laboratory at Cornell, a facility funded by New York State Empire Development Corporation. This research was funded by USDOE contract GO18084. We thank David Wilson and Diane Irwin for providing the clones used to produce the cellulases used in this study.

Appendix A. Supplementary data

Supplementary data to this article can be found online at doi:10.1016/j.bpc.2011.02.003.

References

[1] P. Béguin, J.P. Aubert, The biological degradation of cellulose, FEMS Microbiology Reviews 13 (1994) 25–58.
[2] L.P. Walker, D.B. Wilson, Enzymatic hydrolysis of cellulose: an overview, Bioresource Technology 36 (1991) 3–14.
[3] M. Linder, T.T. Teeri, The roles and function of cellulose-binding domains, Journal of Biotechnology 57 (1997) 15–28.
[4] M. Linder, T.T. Teeri, The cellulose-binding domain of the major cellobiohydrolase of Trichoderma reesei exhibits true reversibility and a high exchange rate on crystalline cellulose, Proceedings of the National Academy of Sciences of the United States of America 93 (1996) 12251.
[5] M. Bothwell, Binding capacities for Thermomonospora fusca E3, E4 and E5, the E3 binding domain, and Trichoderma reesei CBHI on Avicel and bacterial microcrystalline cellulose, Bioresource Technology 60 (1997) 169–178.
[6] G. Beldman, A.G.J. Voragen, F.M. Rombouts, M.F. Searle-van Leeuwen, W. Pilnik, Adsorption and kinetic behavior of purified endoglucanases and exoglucanases fromTrichoderma viride, Biotechnology and Bioengineering 30 (1987) 251–257.
[7] D.L. Watson, D.B. Wilson, L.P. Walker, Synergism in binary mixtures of Thermobifida fusca cellulases Cel6B, Cel9A, and Cel5A on BMCC and Avicel, Applied Biochemistry and Biotechnology 101 (2002) 97–111.
[8] H. Jung, D.B. Wilson, L.P. Walker, Binding and reversibility ofThermobifida fusca Cel5A, Cel6B, and Cel48A and their respective catalytic domains to bacterial microcrystalline cellulose, Biotechnology and Bioengineering 84 (2003) 151–159.
[9] N. Santhanam, L.P. Walker, A high-throughput assay to measure cellulase binding and synergism in ternary mixtures, Biological Engineering 1 (2008) 1–19.
[10] T. Jeoh, D. Wilson, L. Walker, Cooperative and competitive binding in synergistic mixtures of Thermobifida fusca cellulases Cel5A, Cel6B, and Cel9A, Biotechnology Progress 18 (2002) 760–769.
[11] A. Kyriacou, R.J. Neufeld, C.R. MacKenzie, Reversibility and competition in the adsorption ofTrichoderma reesei cellulase components, Biotechnology and Bioengineering 33 (1989) 631–637.
[12] Z. Zhu, N. Sathitsuksanoh, Y. Percival Zhang, Direct quantitative determination of adsorbed cellulase on lignocellulosic biomass with its application to study cellulase desorption for potential recycling, Analyst 134 (2009) 2267.
[13] A. Ma, Q. Hu, Y. Qu, Z. Bai, W. Liu, G. Zhuang, The enzymatic hydrolysis rate of cellulose decreases with irreversible adsorption of cellobiohydrolase I, Enzyme and Microbial Technology 42 (2008) 543–547.
[14] G. Hu, J.A. Heitmann, O.J. Rojas, In situ monitoring of cellulase activity by microgravimetry with a quartz crystal microbalance, Journal of Physical Chemistry B 113 (2009) 14761–14768.
[15] X. Turon, O.J. Rojas, R.S. Deinhammer, Enzymatic kinetics of cellulose hydrolysis: a QCM-D study, Langmuir 24 (2008) 3880–3887.
[16] M. Bothwell, D. Wilson, D. Irwin, L. Walker, Binding reversibility and surface exchange of Thermomonospora fusca E3 and E5 and Trichoderma reesei CBHI, Enzyme and Microbial Technology 20 (1997) 411–417.
[17] J.M. Moran-Mirabal, N. Santhanam, S.C. Corgie, H.G. Craighead, L.P. Walker, Immobilization of cellulose fibrils on solid substrates for cellulase-binding studies through quantitative fluorescence microscopy, Biotechnology and Bioengineering 101 (2008) 1129–1141.
[18] D. Axelrod, D. Koppel, J. Schlessinger, E. Elson, W. Webb, Mobility measurement by analysis of fluorescence photobleaching recovery kinetics, Biophysical Journal 16 (1976) 1055–1069.
[19] J. Lippincott-Schwartz, E. Snapp, A. Kenworthy, Studying protein dynamics in living cells, Nature Reviews Molecular Cell Biology 2 (2001) 444–456.
[20] B. Sprague, J. McNally, FRAP analysis of binding: proper and fitting, Trends in Cell Biology 15 (2005) 84–91.
[21] B.L. Sprague, R.L. Pego, D.A. Stavreva, J.G. McNally, Analysis of binding reactions by fluorescence recovery after photobleaching, Biophysical Journal 86 (2004) 3473–3495.

[22] N.L. Thompson, T.P. Burghardt, D. Axelrod, Measuring surface dynamics of biomolecules by total internal reflection fluorescence with photobleaching recovery or correlation spectroscopy, Biophysical Journal 33 (1981) 435–454.
[23] E.J. Jervis, C.A. Haynes, D.G. Kilburn, Surface diffusion of cellulases and their isolated binding domains on cellulose, Journal of Biological Chemistry 272 (1997) 24016.
[24] E.D. Jung, G. Lao, D. Irwin, B.K. Barr, A. Benjamin, D.B. Wilson, DNA sequences and expression in Streptomyces lividans of an exoglucanase gene and an endoglucanase gene from Thermomonospora fusca, Applied and Environmental Microbiology 59 (1993) 3032–3043.
[25] J.M. Moran-Mirabal, S.C. Corgie, J.C. Bolewski, H.M. Smith, B.R. Cipriany, H.G. Craighead, et al., Labeling and purification of cellulose-binding proteins for high resolution fluorescence applications, Analytical Chemistry 81 (2009) 7981–7987.
[26] P. Thevenaz, U. Ruttimann, M. Unser, A pyramid approach to subpixel registration based on intensity, IEEE Transactions on Image Processing 7 (1998) 27–41.
[27] P. Ross, R. Mayer, M. Benziman, Cellulose biosynthesis and function in bacteria, Microbiology and Molecular Biology Reviews 55 (1991) 35.
[28] M. Deinema, L. Zevenhuizen, Formation of cellulose fibrils by gram-negative bacteria and their role in bacterial flocculation, Archives of Microbiology 78 (2004) 42–57.
[29] W.J. Orts, J. Shey, S.H. Imam, G.M. Glenn, M.E. Guttman, J. Revol, Application of cellulose microfibrils in polymer nanocomposites, Journal of Polymers and the Environment 13 (2005) 301–306.
[30] H.E. Grethlein, The effect of pore size distribution on the rate of enzymatic hydrolysis of cellulosic substrates, Nature Biotechnology 3 (1985) 155–160.
[31] J. Hong, X. Ye, Y.P. Zhang, Quantitative determination of cellulose accessibility to cellulase based on adsorption of a nonhydrolytic fusion protein containing cbm and gfp with its applications, Langmuir 23 (2007) 12535–12540.
[32] Y. Li, D.C. Irwin, D.B. Wilson, Processivity, substrate binding, and mechanism of cellulose hydrolysis by Thermobifida fusca Cel9A, Applied and Environmental Microbiology 73 (2007) 3165–3172.
[33] M. Bothwell, L.P. Walker, Evaluation of parameter estimation methods for estimating cellulase binding constants, Bioresource Technology 53 (1995) 21–29.